

Energy functionals in momentum space: Exchange energy, quantum corrections, and the Kohn-Sham scheme

Marek Cinal*

Instytut Chemii Fizycznej Polskiej Akademii Nauk, ul. Kasprzaka 44/52, PL-01-224 Warszawa, Poland

Berthold-Georg Englert†

Sektion Physik, Universität München, Am Coulombwall 1, D-85748 Garching, Germany

(Received 21 December 1992)

We derive, to leading order, the momentum-space functionals of the exchange energy and of the quantum corrections to the electrostatic energy. The energy functionals thus refined are used to introduce a Kohn-Sham scheme for self-consistent momentum-space calculations. This scheme is applied to helium and beryllium. The results differ from those obtained in the standard Kohn-Sham scheme in configuration space. The total binding energies predicted by the momentum-space computation are somewhat better than those of the configuration-space method.

PACS number(s): 31.15.+q, 31.20.Sy, 31.90.+s

INTRODUCTION

In two recent papers [1,2] we formulated the general theory of energy functionals in momentum space—*momental* functionals, for short. We thereby extended Henderson's [3] proposal, which dealt only with functionals of the momentum density, by introducing the concept of the effective kinetic energy. The tools developed for the corresponding spatial formalism based upon the effective potential energy, reviewed more technically in [4] and [5] and more pedagogically in [6], are then applicable. In [1] and [2] we studied the Thomas-Fermi (TF) and Thomas-Fermi-Scott (TFS) approximations to the momental energy functionals for atoms and found that the spatial and momental TF models are perfectly equivalent, in contrast to the two TFS models, which are not. The latter observation illustrates that analogous physical approximations performed in different contexts need not produce identical results. Indeed, the motivation for developing the momental formalism, as a supplement to the standard spatial one, originates in applications where the spatial formalism, and in particular the spatial Kohn-Sham (KS) scheme, cannot provide for reliable answers. Examples are the computation of momental densities and related quantities such as Compton profiles.

In the present contribution we go beyond the TF and TFS approximations of [1] and [2] by including the exchange energy, in the Dirac-Jensen approximation, and quantal corrections to the direct electrostatic interaction energy into the momental energy functional. We then proceed to the momental KS scheme, hinted at briefly in [1], which we apply to helium and beryllium. We observe differences between the momental densities inferred from the standard spatial KS scheme and those obtained self-consistently in the new momental KS scheme. For both helium and beryllium these differences are marked.

The total binding energies obtained in the two KS

schemes are different, too. We find that the spatial KS scheme underestimates the binding energies, whereas the momental KS scheme overestimates them. The numbers are in favor of the momental scheme, inasmuch as the errors in the energies it produces are smaller than the corresponding errors in the spatial scheme.

A momental KS code that will be capable of dealing with more complicated atoms is being developed and results will be reported in due course. We use atomic units throughout and employ the notational conventions of [1] and [4].

EXCHANGE

The exchange energy

$$E_{\text{ex}} = -\frac{1}{4} \int (d\mathbf{r}') (d\mathbf{r}'') \frac{n(\mathbf{r}'; \mathbf{r}'') n(\mathbf{r}''; \mathbf{r}')}{|\mathbf{r}' - \mathbf{r}''|} \quad (1)$$

acquires a more useful form upon expressing the spatial one-particle density matrix $n(\mathbf{r}'; \mathbf{r}'')$ in terms of the corresponding Wigner function $\nu(\mathbf{r}', \mathbf{p}')$,

$$n(\mathbf{r}'; \mathbf{r}'') = \int \frac{(d\mathbf{p}')}{(2\pi)^3} \nu \left[\frac{\mathbf{r}' + \mathbf{r}''}{2}, \mathbf{p}' \right] e^{i\mathbf{p}' \cdot (\mathbf{r}' - \mathbf{r}'')}, \quad (2)$$

viz.,

$$E_{\text{ex}} = -\pi \int (d\mathbf{r}') \frac{(d\mathbf{p}')}{(2\pi)^3} \frac{(d\mathbf{p}'')}{(2\pi)^3} \times \frac{\nu(\mathbf{r}', \mathbf{p}') \nu(\mathbf{r}', \mathbf{p}'')}{(\mathbf{p}' - \mathbf{p}'')^2}. \quad (3)$$

Let us note in passing that Dirac himself in his seminal 1930 paper [7] made use of a phase-space distribution that was later named the "Wigner function" after Wigner's paper [8] appeared in 1932. To find the Dirac-Jensen [7,9] approximations to E_{ex} we have to insert the TF approximation to the Wigner function, given by

$$v(\mathbf{r}', \mathbf{p}') = 2\eta\{[3\pi^2 n(\mathbf{r}')]^{1/3} - p'\} \quad (4)$$

if the dependence on the spatial density $n(\mathbf{r}')$ is emphasized, or by

$$v(\mathbf{r}', \mathbf{p}') = 2\eta\{[3\pi^2 \rho(\mathbf{p}')]^{1/3} - r'\} \quad (5)$$

if the dependence on the momental density $\rho(\mathbf{p}')$ is focused upon. In (4) and (5), $\eta(x)$ denotes Heaviside's unit step function, and the factors of 2 account for the spin multiplicity.

In view of the common \mathbf{r}' argument of the two Wigner functions in (3), the step functions in (4) and (5) imply

$$v(\mathbf{r}', \mathbf{p}')v(\mathbf{r}', \mathbf{p}'') = \begin{cases} 4\eta\{[3\pi^2 n(\mathbf{r}')]^{1/3} - p_>\} & \text{for (4)} \\ 4\eta\{[3\pi^2 \rho_<]^{1/3} - r'\} & \text{for (5)}, \end{cases} \quad (6)$$

where $p_> = \max\{p', p''\}$ and $\rho_< = \min\{\rho(\mathbf{p}'), \rho(\mathbf{p}'')\}$. One can then either perform the two momentum integrations in (3) or the one remaining spatial integration. The outcomes are

$$E_{\text{ex}}[n] = -\frac{1}{4\pi^3} \int (d\mathbf{r}') [3\pi^2 n(\mathbf{r}')]^{4/3}, \quad (7)$$

which is the familiar spatial Dirac-Jensen functional, and

$$\tilde{E}_{\text{ex}}[\rho] = -\frac{1}{4\pi^2} \int (d\mathbf{p}') (d\mathbf{p}'') \frac{\rho_<}{(\mathbf{p}' - \mathbf{p}'')^2}, \quad (8)$$

which is the corresponding new momental exchange-energy functional. For a momental density that is spherical symmetric, $\rho(\mathbf{p}') = \rho(p')$, and monotonically decreasing, $\rho_< = \rho(p_>)$, the latter functional has the strikingly simple form

$$\tilde{E}_{\text{ex}}[\rho] = -\frac{1}{\pi} \int (d\mathbf{p}') p' \rho(p'). \quad (9)$$

Incidentally we note that this states that the coefficient B_0 of [10] equals $1/\pi = 0.3183$, about two percent more than the value found there by numerical data fitting.

As a check we evaluate (8), or (9), perturbatively by inserting the momental density obtained in the TF approximation [1],

$$\rho(p') = \frac{1}{3\pi^2} r'^3 \quad (10)$$

with r' determined by

$$V(r') + \xi = -\frac{1}{2} p'^2, \quad (11)$$

where $V(r')$ is the corresponding effective TF potential and ξ is the negative of the chemical potential. A change of the integration variable from \mathbf{p}' to \mathbf{r}' reproduces the known answer [11,12]

$$E_{\text{ex}} = -\frac{1}{4\pi^3} \int (d\mathbf{r}') \{-2[V(r') + \xi]\}^2, \quad (12)$$

in which the domain of integration is the classically allowed region where $V + \xi$ is negative. One usually arrives at (12) by employing the TF result

$$n(\mathbf{r}') = \frac{1}{3\pi^2} \{-2[V(r') + \xi]\}^{3/2} \quad (13)$$

in (7). Here the square root of negative arguments is zero by convention.

The exchange energy functionals (7) and (8) suffer from analogous insufficiencies. The spatial one overestimates the exchange energy in the low-density region of large r' . Correspondingly, the momental functional (8) overestimates the contribution from the small- p' range where $\rho(\mathbf{p}')$ is large. These features are particularly obvious in the two Thomas-Fermi-Dirac (TFD) functionals that one obtains by adding $E_{\text{ex}}[n]$ of (7) or $\tilde{E}_{\text{ex}}[\rho]$ of (9) to the two TF functionals, given in Eqs. (59) and (60) of [1], respectively. Both TFD functionals are inconsistent, unless one confines the spatial density $n(\mathbf{r}')$ to the interior of a r' sphere and the momental density $\rho(\mathbf{p}')$ to the exterior of a p' sphere with a corresponding radius. In this way, the troublesome large- r' and small- p' regions are explicitly excluded by hand. In return one has to accept that the densities are discontinuous at these artificial boundaries. Their locations are, of course, not uniquely determined but merely restricted to corresponding ranges, within which each value is equally acceptable [13]. The spatial TFD model thus constructed is then perfectly equivalent to the corresponding momental TFD model, as can be demonstrated analogously to the related discussion in [1] that concerns the equivalence of the two TF models.

In addition to this mathematical inconsistency of the TFD approximation there is also a physical one. The exchange energy contributes nine-elevenths to the $Z^{5/3}$ term in the total atomic binding energy (the leading TF term is proportional to $Z^{7/3}$), the remaining two-elevenths are supplied by quantum corrections [12] that improve upon the TF evaluation of the independent-particle energy, denoted by $E_1[V + \xi]$ and $\tilde{E}_1[T + \xi]$ in [1], and also—in the momental formalism—the evaluation of the direct electrostatic interaction energy. Including only exchange into the description but not also the quantum corrections is, therefore, physically unreasonable—not to mention the left-out Scott correction [11,14,2], which is of order Z^2 . These difficulties are avoided, at least to a large extent, by not evaluating the independent-particle energies semiclassically at all, but rather fully quantum mechanically, which unfortunately can only be done numerically. This is achieved by the KS schemes, the standard spatial one and the momental one.

QUANTUM CORRECTIONS

As mentioned, consistency requires the inclusion of quantal corrections into the momental functional $\tilde{E}_{\text{es}}[\rho]$ of the direct electrostatic energy. It is expedient to express the electrostatic energy

$$E_{\text{es}} = \frac{1}{2} \int (d\mathbf{r}') (d\mathbf{r}'') \frac{n(\mathbf{r}')n(\mathbf{r}'')}{|\mathbf{r}' - \mathbf{r}''|} \quad (14)$$

with the aid of the Wigner function introduced in (2),

$$\begin{aligned} \tilde{E}_{\text{es}}[\rho] &= \frac{1}{2} \int \frac{(d\mathbf{p}')}{(2\pi)^3} \frac{(d\mathbf{p}'')}{(2\pi)^3} \\ &\quad \times \int (d\mathbf{r}') (d\mathbf{r}'') \frac{v(\mathbf{r}', \mathbf{p}')v(\mathbf{r}'', \mathbf{p}'')}{|\mathbf{r}' - \mathbf{r}''|}. \end{aligned} \quad (15)$$

One easily confirms that the TF approximation (5) to ν yields the TF approximation to \tilde{E}_{es} ,

$$\tilde{E}_{\text{es}}^{\text{TF}}[\rho] = \frac{3}{4}(3\pi^2)^{-1/3} \int (d\mathbf{p}') (d\mathbf{p}'') [\rho_{>}^{2/3} \rho_{<} - \frac{1}{5} \rho_{<}^{5/3}] ; \quad (16)$$

this is Eq. (58) of [1].

The leading quantum correction $\Delta_{\text{qu}}\nu$ to $\nu(\mathbf{r}', \mathbf{p}')$ is derived in the Appendix. It amounts to replacing (5) by

$$\begin{aligned} \nu(\mathbf{r}', \mathbf{p}') &= 2\eta(R - r') + \frac{1}{36} \left[\frac{\partial}{\partial \mathbf{r}'} \right]^2 \\ &\quad \times \delta \left[\frac{1}{r'} - \frac{1}{R} \right] \left[\frac{\partial}{\partial \mathbf{p}'} \right]^2 \frac{1}{R} \\ &\equiv \nu^{\text{TF}} + \Delta_{\text{qu}}\nu, \end{aligned} \quad (17)$$

where $R = R(\mathbf{p}') \equiv [3\pi^2 \rho(p')]^{1/3}$. We note that the spherical symmetry of the atom has been explicitly used in the derivation of (17). The resulting correction to \tilde{E}_{es} is

$$\Delta_{\text{qu}}\tilde{E}_{\text{es}}[\rho] = -\frac{1}{48\pi^2} \int (d\mathbf{p}') (d\mathbf{p}'') \rho_{<}^{4/3} \nabla^2 \rho_{<}^{-1/3} \quad (18)$$

with $\nabla \equiv \partial/\partial \mathbf{p}$. In the TF regime one has $p \sim Z^{2/3}$ and $\rho \sim Z^{-3/3}$, so that $\tilde{E}_{\text{es}}^{\text{TF}} \sim Z^{7/3}$, whereas $\tilde{E}_{\text{ex}} \sim Z^{5/3}$ and, indeed, $\Delta_{\text{qu}}\tilde{E}_{\text{es}} \sim Z^{5/3}$.

Partial integrations turn (18) into the equivalent expression

$$\Delta_{\text{qu}}\tilde{E}_{\text{es}}[\rho] = \frac{1}{9\pi^2} \int (d\mathbf{p}') (d\mathbf{p}'') \left[\frac{1}{16} \nabla^2 \rho_{<} - \frac{1}{3} (\nabla \sqrt{\rho_{<}})^2 \right]. \quad (19)$$

If the density $\rho(p')$ is monotonically decreasing, $\rho_{<} \equiv \rho(p_{>})$, this simplifies to

$$\Delta_{\text{qu}}\tilde{E}_{\text{es}}[\rho] = \frac{2}{9\pi} \int (d\mathbf{p}') \left[p' \rho(p') - \frac{4}{5} p'^3 \left[\frac{\partial}{\partial p'} \sqrt{\rho(p')} \right]^2 \right]. \quad (20)$$

Please observe that the first term compensates for two-ninths of the exchange energy (9).

In summary, the total momental functional $\tilde{E}_{ee}[\rho]$ of the electron-electron interaction energy, in a consistent approximation to order $Z^{5/3}$, is given by the sum of (16), (19) [or (20)], and (8) [or (9)],

$$\begin{aligned} \tilde{E}_{ee}[\rho] &= \tilde{E}_{\text{es}}^{\text{TF}}[\rho] + \Delta_{\text{qu}}\tilde{E}_{\text{es}}[\rho] + \tilde{E}_{\text{ex}}[\rho] \\ &= \frac{1}{4\pi^2} \int (d\mathbf{p}') (d\mathbf{p}'') \left[[(3\pi^2 \rho_{>})^{2/3} - \frac{1}{5} (3\pi^2 \rho_{<})^{2/3}] \rho_{<} + \frac{1}{36} \nabla^2 \rho_{<} - \frac{4}{27} (\nabla \sqrt{\rho_{<}})^2 - \frac{\rho_{<}}{(p' - p'')^2} \right], \end{aligned} \quad (21)$$

or, for monotonic densities,

$$\begin{aligned} \tilde{E}_{ee}[\rho] &= \frac{3}{4} (3\pi^2)^{-1/3} \int (d\mathbf{p}') (d\mathbf{p}'') [\rho(p_{<})]^{2/3} \rho(p_{>}) \\ &\quad - \frac{1}{3\pi} \int (d\mathbf{p}') \left[\frac{2}{5} (3\pi^2)^{2/3} p'^3 [\rho(p')]^{5/3} + \frac{7}{3} p' \rho(p') + \frac{8}{27} p'^3 \left[\frac{\partial}{\partial p'} \sqrt{\rho(p')} \right]^2 \right]. \end{aligned} \quad (22)$$

The analogous spatial functional is, of course,

$$\begin{aligned} E_{ee}[n] &= E_{\text{es}}[n] + E_{\text{ex}}[n] \\ &= \frac{1}{2} \int (d\mathbf{r}') (d\mathbf{r}'') \frac{n(\mathbf{r}') n(\mathbf{r}'')}{|\mathbf{r}' - \mathbf{r}''|} \\ &\quad - \frac{1}{4\pi^3} \int (d\mathbf{r}') [3\pi^2 n(\mathbf{r}')]^{4/3}. \end{aligned} \quad (23)$$

Note that these functionals obey the expected scaling laws

$$\begin{aligned} \tilde{E}_{ee}[\rho_\mu] &= \mu \tilde{E}_{ee}[\rho], \\ E_{ee}[n_\mu] &= \mu E_{ee}[n] \end{aligned} \quad (24)$$

for

$$\begin{aligned} \rho_\mu(\mathbf{p}') &= \mu^{-3} \rho(\mathbf{p}'/\mu), \\ n_\mu(\mathbf{r}') &= \mu^3 n(\mu \mathbf{r}'). \end{aligned} \quad (25)$$

The momental functional must scale like this for all $\mu > 0$ (see [1]), whereas the spatial one is required to do so only in the vicinity of $\mu = 1$ (see [15]).

A comment is in order. In Eq. (17) the leading quantum correction of relative order $Z^{-2/3}$ is taken into account, but the Scott correction is left out, although it (superficially) appears to be of relative order $Z^{-1/3}$. The approximation (17) is tailored, of course, to the evaluation of (15), where the Scott correction is irrelevant. Indeed, the electrostatic interaction energy of the electrons E_{es} remains unchanged by the Scott correction, which affects only the kinetic energy of the electrons and their interaction energy with the nuclear charge. This is well known in the spatial formalism [16]. To show that it remains true in the momental formalism, we remark that the Scott correction would amount to replacing ρ by $\rho - \Delta_s \rho$ on the right-hand side of Eq. (16), where $\Delta_s \rho(p')$ equals Z^{-3} times a function of p'/Z [2,17], in contrast to $\rho(p')$, which is (roughly) equal to Z^{-1} times a function

of $p'/Z^{2/3}$. When keeping these different scaling properties in mind and recalling that $\Delta_s \rho(p')$ is only relevant for large p' , then one finds that the resulting extra terms in \bar{E}_{es} are at most of relative order $Z^{-4/3}$ and, therefore, quite irrelevant. In short, there is no Scott correction to $\bar{E}_{es}[\rho]$.

Another remark concerns the electrostatic self-energy contained in (14). It is compensated for by the self-exchange energy which is part of (1). Therefore, the functionals (21) and (23) are free of any self-energy—at least within the range of validity of the approximations used. Thus, for the helium atom, in which no physical exchange energy is present, the exchange energy contributions to (21) and (23) are pure self-energies. They must be taken into account, nevertheless, because they are needed as compensation for the unphysical electrostatic self-energy.

KOHN-SHAM SCHEMES

The approximate functionals (21) and (23) do not account for correlation energies, which are roughly proportional to $Z^{4/3}$, and therefore it is consistent to disregard as well all correlation contributions to the independent-particle energies. In other words, we shall use the noninteracting-electron approximations for the independent-particle energies, as given in Eqs. (23) and (41) of [1]. The functionals of the total energy are thus

$$\begin{aligned} \tilde{E}[T, \rho, \xi] = & \text{tr}[(\tilde{H} + \xi)\eta(-\tilde{H} - \xi)] \\ & - \int (d\mathbf{p}') [T(\mathbf{p}') - \frac{1}{2}p'^2] \rho(\mathbf{p}') \\ & + \tilde{E}_{ee}[\rho] - \xi N \end{aligned} \quad (26)$$

for the momentum-space formalism, and

$$\begin{aligned} E[V, n, \xi] = & \text{tr}[(H + \xi)\eta(-H - \xi)] \\ & - \int (d\mathbf{r}') \left[V(\mathbf{r}') + \frac{Z}{r'} \right] n(\mathbf{r}') \\ & + E_{ee}[n] - \xi N \end{aligned} \quad (27)$$

for the configuration-space formalism. The trace tr includes a factor of 2 for the spin multiplicity.

The respective independent-particle Hamilton operators

$$\tilde{H} = T(\mathbf{p}) - \frac{Z}{r} \quad (28)$$

and

$$H = \frac{1}{2}\mathbf{p}^2 + V(\mathbf{r}) \quad (29)$$

involve the effective kinetic energy $T(\mathbf{p})$ or the effective potential energy $V(\mathbf{r})$. Their eigenstates $|\tilde{\varphi}_v\rangle$ and $|\varphi_v\rangle$ are the KS orbitals, the eigenvalues $\tilde{\mathcal{E}}_v$ and \mathcal{E}_v are the KS energies:

$$\begin{aligned} \tilde{H}|\tilde{\varphi}_v\rangle &= |\tilde{\varphi}_v\rangle \tilde{\mathcal{E}}_v, \\ H|\varphi_v\rangle &= |\varphi_v\rangle \mathcal{E}_v. \end{aligned} \quad (30)$$

Inasmuch as \tilde{H} does not commute with H , the respective

eigenstates and eigenvalues are not identical.

Since the analytical properties of $T(\mathbf{p})$ and $V(\mathbf{r})$ are rather unknown, it is natural to use momental wave functions $\tilde{\varphi}_v(\mathbf{p}') = \langle \mathbf{p}' | \tilde{\varphi}_v \rangle$ and spatial wave functions $\varphi_v(\mathbf{r}') = \langle \mathbf{r}' | \varphi_v \rangle$, respectively. The eigenvalue equations (30) are then turned into a less-familiar momental integral equation,

$$[T(\mathbf{p}') - \tilde{\mathcal{E}}_v] \tilde{\varphi}_v(\mathbf{p}') = \frac{Z}{2\pi^2} \int (d\mathbf{p}'') \frac{\tilde{\varphi}_v(\mathbf{p}'')}{(\mathbf{p}' - \mathbf{p}'')^2}, \quad (31)$$

and a quite-familiar spatial differential equation,

$$[V(\mathbf{r}') - \mathcal{E}_v] \varphi_v(\mathbf{r}') = \frac{1}{2} \left[\frac{\partial}{\partial \mathbf{r}'} \right]^2 \varphi_v(\mathbf{r}'). \quad (32)$$

Note that the two KS wave functions appearing here are not Fourier transforms of each other:

$$\tilde{\varphi}_v(\mathbf{p}') \neq \varphi_v(\mathbf{p}') = \langle \mathbf{p}' | \varphi_v \rangle = \int (d\mathbf{r}') \frac{e^{-i\mathbf{p}' \cdot \mathbf{r}'}}{(2\pi)^{3/2}} \varphi_v(\mathbf{r}'). \quad (33)$$

Therefore, the momental density inferred from the spatial KS wave functions $\varphi_v(\mathbf{r}')$, via their Fourier transforms $\varphi_v(\mathbf{p}')$, will be different from the self-consistently-determined momental density, constructed from the momental KS wave functions $\tilde{\varphi}_v(\mathbf{p}')$.

The stage is now set for a presentation of the KS schemes. We begin with the standard spatial one [18]. The stationary property of the energy functional (27) under variations of V and ξ implies

$$\begin{aligned} n(\mathbf{r}') &= \frac{\delta}{\delta V(\mathbf{r}')} \text{tr}[(H + \xi)\eta(-H - \xi)] \\ &= 2 \langle \mathbf{r}' | \eta(-H - \xi) | \mathbf{r}' \rangle \\ &= 2 \sum_v |\varphi_v(\mathbf{r}')|^2 \eta(-\mathcal{E}_v - \xi) \end{aligned} \quad (34)$$

and

$$\begin{aligned} N &= \frac{\partial}{\partial \xi} \text{tr}[(H + \xi)\eta(-H - \xi)] = \text{tr} \eta(-H - \xi) \\ &= 2 \sum_v \eta(-\mathcal{E}_v - \xi). \end{aligned} \quad (35)$$

For a given effective potential V , Eq. (35) determines which KS orbitals contribute to the sum in (34) such that the count of electrons equals the preassigned value N . Then (34) supplies the spatial density of that given $V(\mathbf{r})$. On the other hand, the stationary property of (27) under variations of n implies

$$V(\mathbf{r}') = -\frac{Z}{r'} + \frac{\delta}{\delta n(\mathbf{r}')} E_{ee}[n] = -\frac{Z}{r'} + V_{ee}(\mathbf{r}'), \quad (36)$$

where the interaction contribution is given by

$$V_{ee}(\mathbf{r}') = \int (d\mathbf{r}'') \frac{n(\mathbf{r}'')}{|\mathbf{r}' - \mathbf{r}''|} - \frac{1}{\pi} [3\pi^2 n(\mathbf{r}')]^{1/3} \quad (37)$$

if $E_{ee}[n]$ of (23) is referred to. Equation (36) tells us the

effective potential when the spatial density is known. The self-consistent circle is now complete.

The well-known spatial KS scheme is a self-consistent iteration that begins with an initial guess for $V(\mathbf{r})$, for which the KS orbitals φ_v have to be found from the differential equation (32) along with their eigenvalues \mathcal{E}_v . Then (34) and (35) produce the spatial density n , which is inserted, via (37), into (36) to yield an improved effective potential. This procedure is repeated as often as necessary to reach the desired accuracy. With V , n , and ζ thus determined the various contributions to the total energy (27) can be evaluated, among them

$$E_{\text{IP}} \equiv \text{tr}[(H + \zeta)\eta(-H - \zeta)] - \zeta N = 2 \sum_v \mathcal{E}_v \eta(-\mathcal{E}_v - \zeta), \quad (38)$$

an explicit sum over the independent-particle energies.

The analogous equations for the new momental KS

scheme result from the stationary property of the momental energy functional (26) under variations of T , ζ , and ρ , viz.,

$$\begin{aligned} \rho(\mathbf{p}') &= \frac{\delta}{\delta T(\mathbf{p}')} \text{tr}[(\tilde{H} + \zeta)\eta(-\tilde{H} - \zeta)] \\ &= 2 \sum_v |\tilde{\varphi}_v(\mathbf{p}')|^2 \eta(-\tilde{\mathcal{E}}_v - \zeta) \end{aligned} \quad (39)$$

and

$$N = \frac{\partial}{\partial \zeta} \text{tr}[(\tilde{H} + \zeta)\eta(-\tilde{H} - \zeta)] = 2 \sum_v \eta(-\tilde{\mathcal{E}}_v - \zeta), \quad (40)$$

as well as

$$T(\mathbf{p}') = \frac{1}{2} p'^2 + \frac{\delta}{\delta \rho(\mathbf{p}')} \tilde{E}_{ee}[\rho] = \frac{1}{2} p'^2 + T_{ee}(\mathbf{p}'). \quad (41)$$

If $\tilde{E}_{ee}[\rho]$ of (22) is used, then the interaction contribution is

$$\begin{aligned} T_{ee}(\mathbf{p}') &= [3\pi^2 \rho(p')]^{1/3} 4\pi \int_{p'}^{\infty} dp'' p''^2 \rho(p'') + \frac{2}{\pi} \int_0^{p'} dp'' p''^2 [3\pi^2 \rho(p'')]^{2/3} - \frac{2}{9\pi} p'^3 [3\pi^2 \rho(p')]^{2/3} - \frac{7}{9\pi} p' \\ &\quad + \frac{2}{81\pi} p' \left[10 \frac{p'}{\rho(p')} \frac{\partial \rho(p')}{\partial p'} - \left(\frac{p'}{\rho(p')} \frac{\partial \rho(p')}{\partial p'} \right)^2 + 2 \frac{p'^2}{\rho(p')} \frac{\partial^2 \rho(p')}{\partial p'^2} \right], \end{aligned} \quad (42)$$

valid for monotonic densities.

The momental KS scheme begins with an initial guess for $T(\mathbf{p}')$, for which the KS orbitals $\tilde{\varphi}_v(\mathbf{p}')$ have to be found from the integral equation (31) along with their eigenvalues $\tilde{\mathcal{E}}_v$. Then (39) and (40) produce the momental density ρ , which is inserted, via (42), into (41) to yield an improved effective kinetic energy. One repeats this procedure until the desired accuracy is reached. With T , ρ , and ζ thus determined self-consistently, one can evaluate the various contributions to the total energy (26), where-by

$$\begin{aligned} \tilde{E}_{\text{IP}} &\equiv \text{tr}[(\tilde{H} + \zeta)\eta(-\tilde{H} - \zeta)] - \zeta N \\ &= 2 \sum_v \tilde{\mathcal{E}}_v \eta(-\tilde{\mathcal{E}}_v - \zeta) \end{aligned} \quad (43)$$

exhibits an explicit sum over the independent-particle energies $\tilde{\mathcal{E}}_v$.

Please observe that the KS orbitals are auxiliary quantities to be used for the sole purpose of evaluating the independent-particle traces that appear in Eqs. (34) and (39), for example. The KS orbitals do not possess a physical significance per se. Neither are they identical with Löwdin's natural orbitals [1], nor is the true many-particle wave function a Slater determinant of KS orbitals. Indeed, the KS schemes do not provide us with information about the many-particle wave function of the atom. To the accuracy of the physical approximations that enter (27), the spatial KS scheme supplies the correct spatial density $n(\mathbf{r}')$ of the ground state and the correct ground-state energy—and nothing else. Likewise, the momental KS scheme supplies the correct momental den-

sity $\rho(\mathbf{p}')$ of the ground state and the correct ground-state energy—nothing more and nothing less. In particular, the spatial KS scheme cannot provide for a truly reliable momental density, although the natural attempt that employs the $\varphi_v(\mathbf{p}')$ of (33) in (39) instead of the $\tilde{\varphi}_v(\mathbf{p}')$,

$$\rho(\mathbf{p}') \cong 2 \sum_v |\varphi_v(\mathbf{p}')|^2 \eta(-\mathcal{E}_v - \zeta), \quad (44)$$

usually produces a reasonable approximation.

We have presented the standard, traditional reasoning, where the starting points are the energy functionals, and the densities are determined self-consistently. It has recently been demonstrated [21–24] that the reverse is possible, too. Provided that the (spatial) density is known, one can find—by more than one method—the (spatial) KS orbitals and also the effective potential (36) for that given density. The KS orbitals thus found for the neutral beryllium atom, based on a theoretical density believed to be accurate, are compared with Hartree-Fock (HF) orbitals in [22] and also with “HF-KS” orbitals, fake KS orbitals generated from the HF density. It is observed that although “the three sets of orbitals are qualitatively similar, they are in fact significantly different” [22]. Neither the similarities nor the differences are unexpected. The HF orbitals are constructed to produce the optimal Slater determinant approximating the true many-particle wave function. The HF density is always at variance with the true density. Consequently, the true KS orbitals cannot be identical with the HF orbitals. Further, we note that HF orbitals are essentially unique, whereas the present work shows that there is more than one set of equally

consistent KS orbitals, quite different sets as a matter of fact, in view of the unequal sign in (33). It would be interesting to see if methods analogous to those of [21–24] can be used to find the momental KS orbitals for a known momental density.

NUMERICAL RESULTS

We have applied the momental KS scheme to neutral helium and neutral beryllium. In these atoms, only s orbitals are present, for which (31) simplifies to the one-dimensional integral equation

$$[T(p') - \tilde{\mathcal{E}}_v] \chi_v(p') = \frac{Z}{\pi} \int_0^\infty dp'' \ln \left| \frac{p' + p''}{p' - p''} \right| \chi_v(p'') \quad (45)$$

obeyed by the radial wave functions $\chi_v(p') = p' \tilde{\varphi}_v(\mathbf{p}')$. This first, and rather elementary, application served the sole purpose of demonstrating the differences between the momental densities obtained self-consistently in the momental KS scheme and those inferred, via (44), from the spatial KS orbitals. The numerical method used for solving (45) was neither very fast nor highly accurate, though quite sufficient for said present purpose. A much more efficient computer code for momental KS calculations—capable of dealing with more complicated atoms containing also p , d , and f electrons—is in the working.

Figure 1 shows the self-consistently computed effective kinetic energies $t = T/Z^{4/3}$ as functions of $y = p'/Z^{2/3}$. The scaling by these powers of $Z^{1/3}$ facilitates the comparison with the universal TF approximation [1]

$$t^{\text{TF}}(y) = 2 \left[\frac{4}{3\pi} \right]^{2/3} / x, \quad (46)$$

with x related to y by

$$y = 2 \left[\frac{4}{3\pi} \right]^{1/3} \sqrt{F(x)/x}, \quad (47)$$

which involves the neutral-atom TF function $F(x)$. Please note that $t^{\text{KS}}(y=0) > 0$; that is, $T^{\text{KS}}(p'=0) > 0$, for both helium and beryllium. Since $T_{\text{kin}}(p) = \frac{1}{2}p^2$ vanishes for $p=0$, these positive values of T^{KS} originate in the interaction contribution T_{ee} .

For large p' values, the KS density contains the Scott correction, so that $\rho(p') \sim p'^{-8}$ asymptotically as in the TFS model [2]. Consequently, Eq. (42) implies

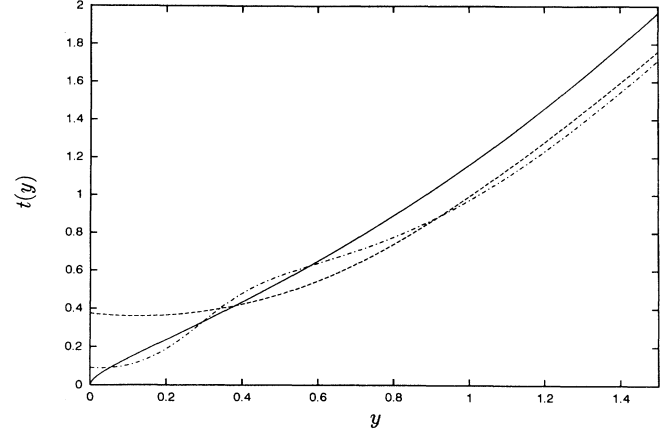


FIG. 1. Effective kinetic energy $T(p')$ for helium (---) and beryllium (-.-.-). The plot actually shows $t = T/Z^{4/3}$ as a function of $y = p'/Z^{2/3}$. The solid line is the universal TF result.

$$T^{\text{KS}}(p') = \frac{1}{2}p'^2 - \frac{7}{9\pi}p' + \frac{1}{2\pi^2} \int (d\mathbf{p}'') [3\pi^2\rho(p'')]^{2/3} + \dots, \quad (48)$$

where the ellipses represent contributions that vanish in the limit $p' \rightarrow \infty$. The p' -independent term equals 4.02 for helium and 9.62 for beryllium. In the TF and TFS models, this term approximates the electrostatic energy \tilde{E}_{Ne} between the nucleus and the electrons according to

$$\frac{1}{2\pi^2} \int (d\mathbf{p}') [3\pi^2\rho(p')]^{2/3} \cong \begin{cases} -\tilde{E}_{Ne}/Z & \text{for TF} \\ Z - \tilde{E}_{Ne}/Z & \text{for TFS;} \end{cases} \quad (49)$$

see Eq. (52) in [1] and Eq. (21) in [2]. The KS values reported for \tilde{E}_{Ne} in Tables I and II give 3.44 (TF) and 5.44 (TFS) for helium as well as 8.37 (TF) and 12.4 (TFS) for beryllium on the right-hand side of (49), in satisfactory agreement with the actual values on the left-hand side.

Further, we note that the effective kinetic energy for the one-shell-atom helium is smooth, whereas that of the two-shell-atom beryllium exhibits oscillations around the TF curve, which one naturally associates with the shell structure.

Let us now turn to the wave functions plotted in Fig. 2. As stated at the end of the preceding section, these wave functions are auxiliary quantities of little interest in

TABLE I. Energies for helium, determined self-consistently in both KS schemes, the momental and the spatial one. The columns list the KS energy of the $1s$ electrons, the independent-particle energy of Eqs. (38) or (43), the kinetic energy, the electrostatic interaction energy between the nucleus and the electrons, the direct electrostatic interaction energy between the electrons (TF contribution only for the momental scheme), the quantum correction to it (momental scheme only), the exchange energy, and the total energy.

Scheme	\mathcal{E}_{1s}	E_{IP}	E_{kin}	E_{Ne}	E_{ee}	E_{es}^{TF}	$\Delta_{\text{qu}}E_{es}$	E_{ex}	E_{total}
Momental	-0.812	-1.62	2.99	-6.89	0.93	2.04	-0.22	-0.91	-2.99
Spatial	-0.517	-1.03	2.72	-6.56	1.12	1.97		-0.85	-2.72

TABLE II. Energies for beryllium, columns labeled as in Table I, except for the additional column for the KS energy of the 2s electrons.

Scheme	\mathcal{E}_{1s}	\mathcal{E}_{2s}	E_{IP}	E_{kin}	E_{Ne}	E_{ee}	E_{es}^{TF}	$\Delta_{qu}E_{es}$	E_{ex}	E_{total}
Momental	-4.63	-0.387	-10.0	14.7	-33.5	4.08	6.96	-0.56	-2.32	-14.7
Spatial	-3.79	-0.170	-7.92	14.2	-33.2	4.77	7.05		-2.28	-14.2

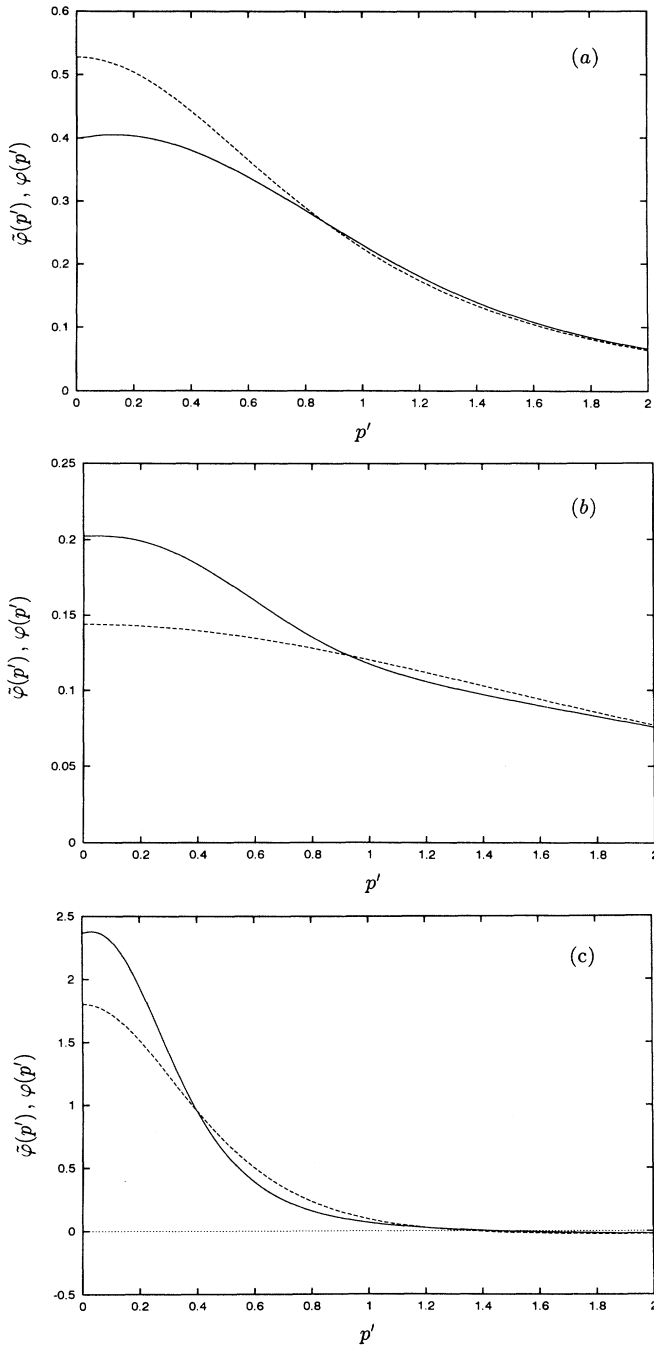


FIG. 2. Momental KS wave functions $\bar{\varphi}(p')$ for (a) helium, 1s state; (b) beryllium, 1s state; (c) beryllium, 2s state. The dashed lines show the Fourier transforms $\varphi(p')$ of the corresponding spatial KS wave functions $\varphi(r')$.

themselves. Nevertheless, it is worth observing that the momental KS wave functions $\bar{\varphi}(p')$ differ substantially from the Fourier transforms $\varphi(p')$ of the spatial KS wave functions. The unequal sign in (33) is convincingly confirmed. The corresponding KS energies in Tables I and II have little in common, too.

As a consequence of the differing wave functions, the resulting momental densities are also at variance. This is demonstrated in Fig. 3, where we plot the radial densities $4\pi p'^2 \rho(p')$ rather than $\rho(p')$ itself, because the beryllium shells are only visible in the radial density.

The Compton profiles

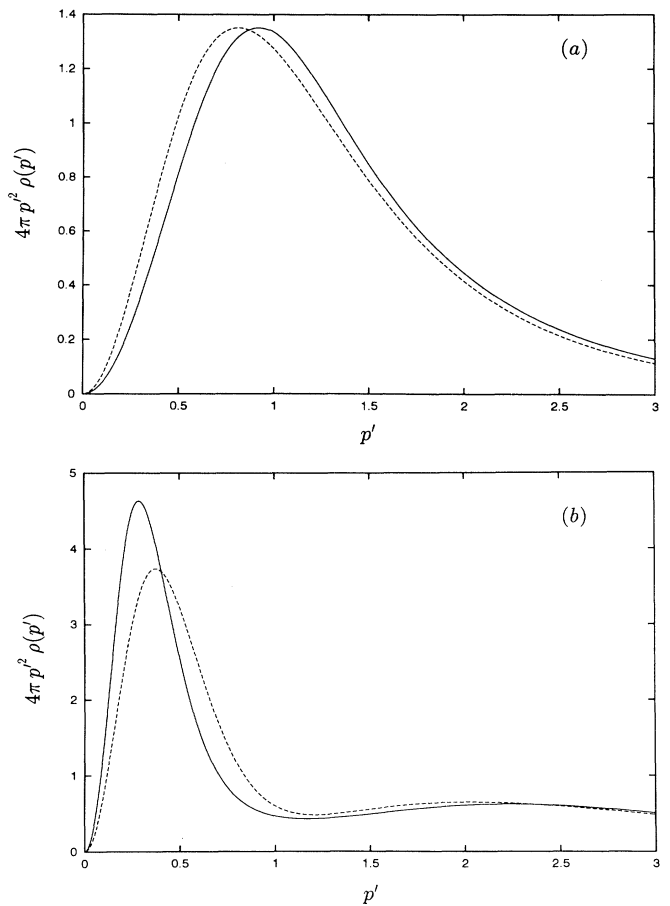


FIG. 3. Radial momental densities $4\pi p'^2 \rho(p')$ for (a) helium and (b) beryllium. The solid lines show the self-consistent densities of the momental KS scheme, and the dashed lines show the approximations inferred in the spatial KS scheme with the aid of Eq. (44).

$$J(q) = \left\langle \frac{\eta(p^2 - q^2)}{2p} \right\rangle = 2\pi \int_{|q|}^{\infty} dp' p' \rho(p') \quad (50)$$

are shown in Fig. 4. Of course, the differences seen in Figs. 2 and 3 are here manifest, too. Since Compton profiles can be determined experimentally, the question arises whether experimental data could tell us which theoretical prediction is better. At the present stage of the development, however, it is still too early for that, because both the momental and the spatial energy functionals are rather crude approximations in the small- p range, where the differences between the two Compton profiles are largest. It is quite possible that the gaps in Figs. 2–4 narrow when better functionals are employed.

The energy values reported in Tables I and II can be checked for consistency in various ways [25]. First, the virial theorem requires that the kinetic energy equals the binding energy, that is, the negative of the total energy. We have used this as a natural control for the accuracy of our numerical procedure and have confidence in the digits given in the tables. More subtle are the relations that express to which extent the interaction of each electron pair is counted multiply in the sum of the independent-particle energies, viz.

$$\tilde{E}_{\text{total}} \equiv \tilde{E} = \tilde{E}_{\text{IP}} - \frac{2}{3} \tilde{E}_{\text{es}}^{\text{TF}} \quad (51)$$

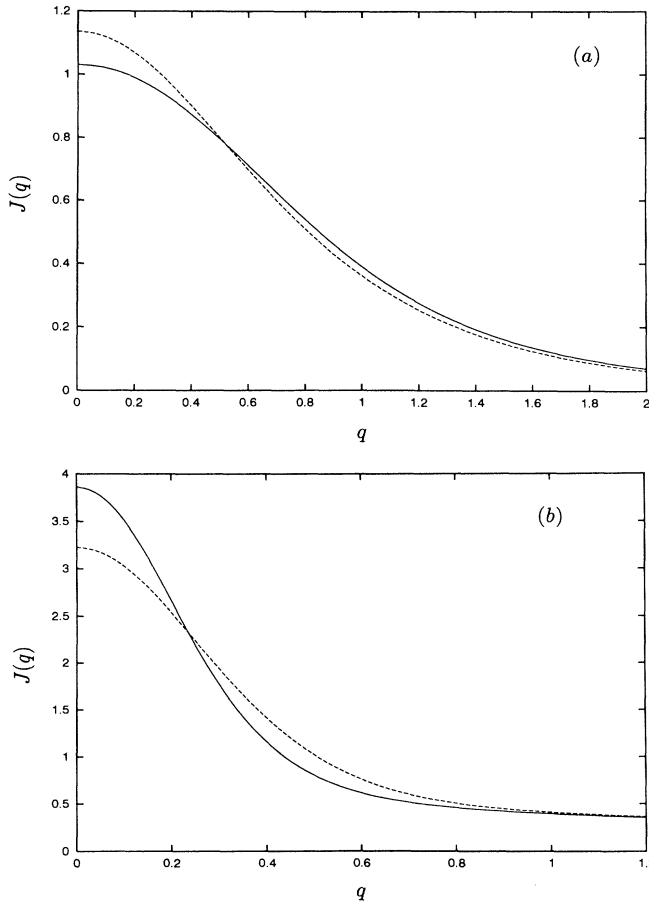


FIG. 4. Compton profiles $J(q)$ to the densities in Fig. 3.

for the momental KS energies, and

$$E_{\text{total}} \equiv E = E_{\text{IP}} - E_{\text{es}} - \frac{1}{3} E_{\text{ex}} \quad (52)$$

for the spatial ones. Both are obeyed quite well by the respective numbers in the tables. A derivation of (51) begins with the observation that, in view of the various powers of ρ that enter the functionals $\tilde{E}_{\text{es}}^{\text{TF}}$ and $\tilde{E}_{\text{ex}} + \Delta_{\text{qu}} \tilde{E}_{\text{es}}$, the identity

$$\begin{aligned} \int (d\mathbf{p}') \rho(\mathbf{p}') [T(\mathbf{p}') - \frac{1}{2} p'^2] &= \int (d\mathbf{p}') \rho(\mathbf{p}') \\ &\times \frac{\delta}{\delta \rho(\mathbf{p}')} \tilde{E}_{\text{ee}}[\rho] \\ &= \frac{5}{3} \tilde{E}_{\text{ee}}^{\text{TF}} + \tilde{E}_{\text{ex}} + \Delta_{\text{qu}} \tilde{E}_{\text{es}} \quad (53) \end{aligned}$$

is obeyed by the actual ρ and T . In conjunction with the definition of the independent-particle energy \tilde{E}_{IP} in (38), this implies (51). Likewise, proceeding from

$$\begin{aligned} \int (d\mathbf{r}') n(\mathbf{r}') [V(\mathbf{r}') + Z/r'] &= \int (d\mathbf{r}') n(\mathbf{r}') \\ &\times \frac{\delta}{\delta n(\mathbf{r}')} E_{\text{ee}}[n] \\ &= 2E_{\text{es}} + \frac{4}{3} E_{\text{ex}} \quad (54) \end{aligned}$$

one establishes (52).

Both KS schemes are self-consistent and involve analogous physical approximations. So the two schemes are equally good in the first place, although they are not perfectly equivalent. For instance, the two schemes produce different predictions for the total binding energies. Both the comparison with the experimental binding energies (helium, 2.9038 a.u.; beryllium, 14.669 a.u.) and with the nonrelativistic HF predictions (helium, 2.8617 a.u.; beryllium, 14.573 a.u.) show that the spatial KS scheme underestimates the binding energy, whereas the momental one overestimates it. The momental-scheme numbers are much closer to the experimental values. The fairer comparison, though, is with the HF results; for helium the HF energy is half-way between the two KS numbers; for beryllium, however, the comparison is clearly in favor of the binding energy predicted by the momental KS scheme.

This observation should not induce the reader into believing that the momental KS scheme generally outperforms the spatial one. Indeed, the momental density and the Compton profile of beryllium calculated from the HF wave functions [26] resemble more the ones obtained in the spatial KS scheme than those of the momental one. In view of the structural similarities between the HF equations and those of the spatial KS scheme, this resemblance is not surprising.

HF results are approximate themselves, of course, they cannot be used as an absolute criterion for judging the quality of approximate spatial or momental functionals. The purpose of the KS schemes is not the reproduction of HF numbers but to provide independent predictions. Indeed, the two KS schemes are independent formulations, independent of each other and also independent of the HF approach.

SUMMARY

We have extended the momentum-space functional method for atomic structure calculations by including both the exchange energy and the quantum corrections to the electrostatic energy. The momental KS scheme that is based upon these refinements has been introduced and applied to helium and beryllium. As expected, we have found that the results are different from those obtained in the standard spatial KS scheme. The quality of the binding energies computed in the momental scheme is not worse than that of the spatial-scheme ones. So we now have not one, but two, KS predictions for the binding energy of each of these atoms; both the experimental values and the HF predictions are sandwiched by the KS numbers.

ACKNOWLEDGMENTS

We would like to thank F. Bell, S. Olszewski, and W. Weyrich for valuable discussions and invaluable encouragement. We are grateful for the technical assistance provided by E. Figge, E. Krönauer, and U. Martini.

APPENDIX

If we denote by $h(\mathbf{r}', \mathbf{p}')$ the Wigner function of an operator $H(\mathbf{r}, \mathbf{p})$, then the TF approximation to the Wigner function $g(\mathbf{r}', \mathbf{p}')$ of an operator function $G(H)$ is given by

$$g(\mathbf{r}', \mathbf{p}') \cong G(h(\mathbf{r}', \mathbf{p}')) . \quad (\text{A1})$$

Quantum corrections to this (highly) semiclassical approximation involve even powers of the two-sided differential operator

$$\Lambda = \frac{\vec{\partial}}{\partial \mathbf{r}'} \cdot \frac{\vec{\partial}}{\partial \mathbf{p}'} - \frac{\vec{\partial}}{\partial \mathbf{p}'} \cdot \frac{\vec{\partial}}{\partial \mathbf{r}'} , \quad (\text{A2})$$

in terms of which the classical Poisson bracket has the compact form

$$g \Lambda h = -h \Lambda g = \frac{\partial g}{\partial \mathbf{r}'} \cdot \frac{\partial h}{\partial \mathbf{p}'} - \frac{\partial g}{\partial \mathbf{p}'} \cdot \frac{\partial h}{\partial \mathbf{r}'} . \quad (\text{A3})$$

Inasmuch as in the TF regime of an atom r' is of the order $Z^{-1/3}$ and $p' \sim Z^{2/3}$, we find $\Lambda \sim Z^{-1/3}$, so that the leading quantum corrections to (A1) are represented by the terms of order Λ^2 . These are exhibited in

$$g(\mathbf{r}', \mathbf{p}') = G(h) - \frac{1}{16} \{ h \Lambda^2 h \} \left[\frac{\partial}{\partial h} \right]^2 G(h) + \frac{1}{24} \{ h \Lambda h \Lambda h \} \left[\frac{\partial}{\partial h} \right]^3 G(h) + \dots , \quad (\text{A4})$$

where Λ acts only upon those functions $h(\mathbf{r}', \mathbf{p}')$ that stand immediately next to it inside the curly brackets, and the ellipses indicate terms that involve at least four factors of Λ .

Consider now a spherically symmetric H of the form

$$H(\mathbf{r}, \mathbf{p}) = v(R(p)) - v(r) , \quad (\text{A5})$$

for which

$$h(\mathbf{r}', \mathbf{p}') = v(R(p')) - v(r') . \quad (\text{A6})$$

Here [$R \equiv R(p')$ everywhere in the sequel]

$$h \Lambda^2 h = -2 \left[\frac{\partial}{\partial \mathbf{r}'} \cdot \frac{\partial}{\partial \mathbf{p}'} \right]^2 v(r') v(R) \quad (\text{A7})$$

and

$$h \Lambda h \Lambda h = \left[\frac{\partial v(R)}{\partial \mathbf{p}'} \cdot \frac{\partial}{\partial \mathbf{r}'} \right]^2 v(r') - \left[\frac{\partial v(r')}{\partial \mathbf{r}'} \cdot \frac{\partial}{\partial \mathbf{p}'} \right]^2 v(R) . \quad (\text{A8})$$

Upon restricting the possible use of (A4) to situations where either a ($d\mathbf{r}'$) or a ($d\mathbf{p}'$) integration is performed, we can average over the angular dependence in (A7) and (A8). This produces the equivalent replacements

$$h \Lambda^2 h \rightarrow -\frac{2}{3} \left[\frac{\partial}{\partial \mathbf{r}'} \right]^2 v(r') \left[\frac{\partial}{\partial \mathbf{p}'} \right]^2 v(R) , \quad (\text{A9})$$

$$h \Lambda h \Lambda h \rightarrow \frac{1}{3} \left[\frac{\partial v(R)}{\partial \mathbf{p}'} \right]^2 \left[\frac{\partial}{\partial \mathbf{r}'} \right]^2 v(r') - \frac{1}{3} \left[\frac{\partial v(r')}{\partial \mathbf{r}'} \right]^2 \left[\frac{\partial}{\partial \mathbf{p}'} \right]^2 v(R) .$$

After rearranging the resulting terms in (A4) we then find that the leading quantum correction to (A1) is

$$g(\mathbf{r}', \mathbf{p}') = G(h) + \frac{1}{72} \left\{ \left[\left[\frac{\partial}{\partial \mathbf{r}'} \right]^2 v(r') \right] \left[\frac{\partial}{\partial \mathbf{p}'} \right]^2 - \left[\left[\frac{\partial}{\partial \mathbf{p}'} \right]^2 v(R) \right] \times \left[\frac{\partial}{\partial \mathbf{r}'} \right]^2 \right\} \frac{\partial}{\partial h} G(h) + \frac{1}{72} \frac{\partial^2 G(h)}{\partial h^2} \left[\frac{\partial}{\partial \mathbf{r}'} \right]^2 v(r') \left[\frac{\partial}{\partial \mathbf{p}'} \right]^2 v(R) . \quad (\text{A10})$$

We regard (5) as corresponding to $v(\mathbf{r}', \mathbf{p}') = g(\mathbf{r}', \mathbf{p}')$ with

$$G(H) = 2\eta \left[-T(p) - \zeta + \frac{Z}{r} \right] = 2\eta [v(R(p)) - v(r)] , \quad (\text{A11})$$

where $v(r') = -Z/r'$, and $R(p')$ is related to the momental density by

$$\rho(\mathbf{p}') = \int \frac{(d\mathbf{r}')}{(2\pi^3)} v(\mathbf{r}', \mathbf{p}') . \quad (\text{A12})$$

In (A10), we then encounter

$$\left[\frac{\partial}{\partial \mathbf{r}'} \right]^2 v(\mathbf{r}') = 4\pi Z \delta(\mathbf{r}'),$$

$$G(h) = 2\eta \left[\frac{Z}{r'} - \frac{Z}{R} \right] = 2\eta(R - r'), \quad (\text{A13})$$

$$\frac{\partial}{\partial h} G(h) = \frac{2}{Z} \delta \left[\frac{1}{r'} - \frac{1}{R} \right] = \frac{1}{2Z} (r' + R)^2 \delta(R - r'),$$

$$\left[\frac{\partial}{\partial h} \right]^2 G(h) = \frac{2}{Z^2} \delta' \left[\frac{1}{r'} - \frac{1}{R} \right]$$

$$= \frac{1}{8Z^2} (r' + R)^4 \delta'(R - r'),$$

$$\left[\left[\frac{\partial}{\partial \mathbf{r}'} \right]^2 v(\mathbf{r}') \right] \frac{\partial}{\partial h} G(h) = 2\pi \delta(\mathbf{r}') (r' + R)^2$$

$$\times \delta(R - r')$$

$$= 8\pi \delta(\mathbf{r}') R^2 \delta(R)$$

$$= 0, \quad (\text{A14})$$

$$\left[\left[\frac{\partial}{\partial \mathbf{r}'} \right]^2 v(\mathbf{r}') \right] \left[\frac{\partial}{\partial h} \right]^2 G(h) = \frac{\pi}{2Z} \delta(\mathbf{r}') (r' + R)^4$$

$$\times \delta'(R - r')$$

$$= \frac{8\pi}{Z} \delta(\mathbf{r}') R^4 \delta'(R)$$

$$= 0.$$

and in particular the vanishing products

As a consequence, (A10) produces (17). We finally note that $\Delta_{\text{qu}} \nu$ in (17) does not contribute to the integral in (A12), so that $\rho(p') = 3\pi^2 [R(p')]^3$.

*Presently at Imperial College, Department of Mathematics, Huxley Building, 180 Queen's Gate, London SW7 2BZ, United Kingdom.

†Also at Max-Planck-Institut für Quantenoptik, Ludwig-Prandtl-Straße 10, D-85748 Garching, Germany.

- [1] B.-G. Englert, Phys. Rev. A **45**, 127 (1992).
- [2] M. Cinal and B.-G. Englert, Phys. Rev. A **45**, 135 (1992).
- [3] G. A. Henderson, Phys. Rev. A **23**, 19 (1981).
- [4] B.-G. Englert, *Semiclassical Theory of Atoms*, Lecture Notes in Physics Vol. 300, edited by J. Ehlers *et al.* (Springer-Verlag, Berlin, 1988).
- [5] I. K. Dmitrieva and G. I. Plindov, *Properties of Atoms and Ions in the Light of the Statistical Theory* (Navuka i Tekhnika, Minsk, 1991) (in Russian).
- [6] L. Spruch, Rev. Mod. Phys. **63**, 151 (1991).
- [7] P. A. M. Dirac, Proc. Cambridge Philos. Soc. **26**, 376 (1930).
- [8] E. Wigner, Phys. Rev. **40**, 749 (1932).
- [9] H. Jensen, Z. Phys. **89**, 713 (1934).
- [10] R. K. Pathak, P. V. Panat, and S. R. Gadre, Phys. Rev. A **26**, 3073 (1982).
- [11] J. M. S. Scott, Philos. Mag. **43**, 859 (1952).
- [12] J. Schwinger, Phys. Rev. A **24**, 2353 (1981).
- [13] This is discussed in a related context by B.-G. Englert and

J. Schwinger, Phys. Rev. A **26**, 2322 (1982); see also Ref. [4], pp. 244–255.

- [14] J. Schwinger, Phys. Rev. A **22**, 1827 (1980).
- [15] M. Levy and J. P. Perdew, Phys. Rev. A **32**, 2010 (1985).
- [16] See, for instance, Ref. [4], pp. 162–164.
- [17] K. Buchwald and B.-G. Englert, Phys. Rev. A **40**, 2738 (1989).
- [18] The spatial KS scheme is discussed extensively in the literature; consult, e.g., the respective chapters in two recent textbooks [19,20].
- [19] R. G. Parr and W. Yang, *Density Functional Theory of Atoms and Molecules* (Oxford University Press, New York, 1989).
- [20] R. M. Dreizler and E. K. U. Gross, *Density Functional Theory* (Springer-Verlag, Berlin, 1990).
- [21] A. Holas and N. H. March, Phys. Rev. A **44**, 5521 (1991).
- [22] Q. Zhao and R. G. Parr, Phys. Rev. A **46**, 2337 (1992).
- [23] Q. Zhao and R. G. Parr, J. Chem. Phys. **98**, 543 (1993). Do not miss footnote 25 in this paper.
- [24] Y. Wang and R. G. Parr, Phys. Rev. A **47**, 1591 (1993).
- [25] Those of our spatial KS numbers that can be compared with the results reported by B. Y. Tong and L. J. Sham, Phys. Rev. **144**, 1 (1966), agree well with their values.
- [26] A. N. Tripathi, R. P. Sagar, R. O. Esquivel, and V. H. Smith, Jr., Phys. Rev. A **45**, 4385 (1992).